Impacts of Quantization on the Properties of Liquid Water

ARTICLE *in* THE JOURNAL OF PHYSICAL CHEMISTRY A · SEPTEMBER 2005

Impact Factor: 2.69 · DOI: 10.1021/jp051616j · Source: PubMed

3 AUTHORS, INCLUDING:

Mohamed Shajahan Gulam Razul
St. Francis Xavier University
13 PUBLICATIONS **164** CITATIONS
SEE PROFILE

Peter G Kusalik
The University of Calgary
114 PUBLICATIONS **3,969** CITATIONS
SEE PROFILE

Impacts of Quantization on the Properties of Liquid Water

L. Hernández de la Peña,† M. S. Gulam Razul, and P. G. Kusalik*

Department of Chemistry, Dalhousie University, Halifax, Nova Scotia B3H 4J3, Canada

Received: March 30, 2005; In Final Form: May 18, 2005

The results of classical and quantum simulations of liquid water over a wide range of temperatures are compared to probe the impact of quantization on the properties of liquid water. We show that, when treated quantum mechanically, water molecules have an enhanced probability of accessing nontetrahedral coordination in the local three-dimensional structure. We discuss how this enhanced probability, also called "effective tunneling", is related to the dynamics of the hydrogen-bond breaking and molecular diffusion in the liquid. We explore in detail how local molecular environments affect the manifestation of quantum effects and identify a previously unreported and apparently unique behavior of the quantum mechanical uncertainty of the water molecule as a function of temperature. The nonmonotonic behavior of the quantum mechanical uncertainty with temperature is shown to be due to the notable strength of the water−water interaction in the condensed phase and becomes further evidence of the importance of the water structure in the properties of this ubiquitous liquid.

I. Introduction

The unique properties of liquid water remain the subject of considerable experimental and theoretical attention, including the relevance of quantum effects. One experimental manifestation of quantum effects in liquid water is the dependence upon isotopic substitution as exemplified[1] by liquid D_2O freezing at 4 °C. According to classical statistical mechanics, H_2O and D_2O should have the same equation of state, and therefore classical simulations with any simple model potential for water will predict identical structural and thermodynamic properties for H_2O and D_2O, in clear contradiction with the experimental evidence. Furthermore, classical simulations are unable to reproduce isotopic effects in the dynamical properties.[2] According to quantum statistical mechanics, however, the uncertainty principle "blurs" the positions of the hydrogens in H_2O more so than for the deuteriums in D_2O and causes the intermolecular interactions in liquid H_2O to be slightly smaller than in (the more classical) D_2O. Quantum mechanics also dictates that there be an uncertainty associated with determining the orientation of any water molecule, henceforth referred to as the quantum mechanical or orientational uncertainty. In this context (i.e., due to the quantum nature of its protons), water is a structurally less ordered liquid when studied quantum mechanically[3−8] than the one predicted by classical simulations. In addition, several authors[7,9,10] have reported an increase of more than 50% in the self-diffusion coefficient in liquid water at 25 °C when quantization is taken into account. In fact, this large increase of the self-diffusion coefficient, sometimes referred to as (or to be due to an) "effective tunneling",[10] has been shown to be even higher at lower temperatures.[11]

Since structure plays a key role in the properties of water, a number of simulation studies[3−7,10] have tried to address the question of local structure in quantum liquid water. These studies, however, have focused only on the limited information provided by differences between the orientationally averaged (or spatially folded) radial distribution functions (e.g., $g_{OO}(r)$) obtained classically and quantum mechanically. Thus, despite clear evidence that quantization affects the properties of liquid water,[1−11] this previous work has not provided a specific explanation for "effective tunneling", and a full account of this behavior has remained illusive. A much more complete understanding of the changes that take place in liquid water structure due to quantization can be obtained by examining the oxygen−oxygen spatial distribution functions (SDFs), $g_{OO}(\mathbf{r})$. SDFs incorporate both the radial and angular components of the interatomic separation vector, **r**, and hence provide spatial maps that fully characterize the local three-dimensional structure in the liquid.[12,13]

In this paper, we examine simulation results for classical and quantum liquid water over a wide range of temperatures and carry out an explicit structural characterization of the "effective tunneling" in liquid H_2O and D_2O. We establish the connection between the changes that take place in the spatial structure of quantum liquid water and the breaking of hydrogen bonds and molecular diffusion of the water molecules in liquid phase. In addition, we perform a detailed analysis of the behavior of the quantum orientational uncertainty with temperature and uncover its relationship with the local molecular environment.

This paper is organized as follows. Section II outlines the details of the simulation methodology we have employed, and our results are presented and discussed in section III. Finally, the conclusions are given in section IV.

II. Computational Methodology

The classical simulations were carried out with a standard molecular dynamics code, and our quantum simulations were based on the centroid molecular dynamics method[14] (CMD) adopted within the rigid body approximation.[10,16] A brief overview of this rigid body-CMD technique is given below.

* To whom correspondence should be addressed. E-mail: Peter.Kusalik@dal.ca.

† Present address: Chemical Physics Theory Group, Department of Chemistry, University of Toronto, Toronto, Ontario M5S 3H6, Canada.

10.1021/jp051616j CCC: $30.25
Published on Web 07/22/2005

The canonical partition function of a rigid quantum object (with a large total mass, m, and small inertia moments, I_x,I_y,I_z) can be written in discretized form as[3,5,10]

$$Z_P(\beta) = \left(\frac{m}{2\pi\beta\hbar^2}\right)^{3/2}\left(\frac{IP}{2\pi\beta\hbar^2}\right)^{3P/2}\int dR\prod_{k=1}^{P}\int d\Omega_k \exp\{-\beta\Phi\} \quad (1)$$

where P is the discretization parameter

$$\Phi = \frac{IP}{2\beta^2\hbar^2}\Gamma^2(\Omega_k,\Omega_{k+1}) + \frac{1}{P}U(R,\Omega_k) \quad (2)$$

and $\Omega_{P+1} = \Omega_1$. In these equations, $I = \sqrt[3]{I_xI_yI_z}$, $\beta = 1/kT$, $\Gamma(\Omega_k,\Omega_{k+1})$ is the rotation angle between the orientations Ω_k and Ω_{k+1}, $U(R,\Omega_k)$ is the classical interaction potential acting on a water molecule, and only the dominant term from the rotational propagator has been retained. Equation 1 can be recast in centroid form as[10,14,16]

$$Z_P(\beta) = \left(\frac{m}{2\pi\beta\hbar^2}\right)^{3/2}\int dR\int d\Omega_c\rho_c(R,\Omega_c) \quad (3)$$

where

$$\rho_c(R,\Omega_c) = \left(\frac{IP}{2\pi\beta\hbar^2}\right)^{3P/2}\prod_{k=1}^{P}\int d\Omega_k\delta(\Omega_c - \Omega_0)\exp\{-\beta\Phi\} \quad (4)$$

is the centroid density, Ω_0, the average bead orientation (see refs 10 and 16), satisfies

$$\min[\sum_{k=1}^{P}\Gamma^2(\Omega_k,\Omega_0)] \quad (5)$$

and Φ is given by eq 2. The CMD method[14] is based on the classical time evolution of the centroid variable on a potential surface which in this case becomes[10,16]

$$V_c(R,\Omega_c) = -\frac{1}{\beta}\ln\rho_c(R,\Omega_c) \quad (6)$$

Hence, the centroid (classical) equations of motion are integrated via molecular dynamics with the use of the centroid force and centroid torque given by

$$F_c(R,\Omega_c) = \frac{-1}{\rho_c(R,\Omega_c)}\left(\frac{IP}{2\pi\beta\hbar^2}\right)^{3P/2}\prod_{k=1}^{P}\int d\Omega_k\delta(\Omega_c - \Omega_0)\left[\frac{1}{P}\sum_{s=1}^{P}\frac{\partial U(R,\Omega_s)}{\partial R}\right]\exp\{-\beta\Phi\} \quad (7)$$

or

$$F_c(R,\Omega_c) = -\left\langle\frac{1}{P}\sum_{s=1}^{P}\frac{\partial U(R,\Omega_s)}{\partial R}\right\rangle_{\{\Omega_k\},\delta(\Omega_c-\Omega_0)} \quad (8)$$

and

$$T_c(R,\Omega_c) = -\left\langle\frac{1}{P}\sum_{s=1}^{P}\frac{\partial\Phi(R,\Omega_s)}{\partial\Omega_s}\right\rangle_{\{\Omega_k\},\delta(\Omega_c-\Omega_0)} \quad (9)$$

respectively. The numerical integration of the centroid constrained orientational averages in eqs 8 and 9 has been described in refs 10 and 16.

It is important to emphasize that the CMD method[14] generates the exact thermodynamic averages of the equilibrium properties (provided that the system is ergodic) as well as very accurate dynamical information for systems where quantum coherence effects are negligible. Therefore, results from CMD allow us to draw the connections between structure and dynamics in a direct manner. This is to be contrasted with the use of equilibrium path integral methods (path integral Monte Carlo, PIMC, or path integral molecular dynamics, PIMD) where no real time dynamical information is available. Furthermore, as will be seen in section III below, one can take advantage of the concept of centroid to analyze the behavior of the quantum mechanical uncertainty.

The present simulations utilize the rigid TIP4P water potential.[17] This model was selected since it is very well characterized and has been demonstrated[12] to reproduce well the local environment in liquid water; it was also chosen because of its computational efficiency. We also remark that in the quantum simulations presented here the TIP4P interaction potential is effectively modified by the inclusion of the orientational uncertainty (see eq 6), and hence its properties (for example its density maximum) are shifted somewhat relative to those obtained from classical simulations.[18] The classical and quantum molecular dynamics simulations were performed with systems of 256 water molecules at constant density. It is important to note that convergence with respect to P, the discretization parameter, has been demonstrated. Moreover, the reliability of the present model and methodology has been confirmed[10] through their ability to reproduce the known isotropic ratios of various properties for liquid water.

III. Results and Discussion

A. The Spatial Structure of Quantum Liquid Water. As has been discussed above, an unambiguous identification of the changes that take place in the local structure of liquid water due to quantization can be carried out with the use of oxygen−oxygen spatial distribution functions (SDFs), $g_{OO}(\mathbf{r}_{ij})$. The analysis of SDFs has been used previously in liquid water[12] and its solutions[13] and has led to a better understanding of the local structure. Kusalik and co-workers[12,13] have clarified a number of structural questions in liquid water by examining in detail the oxygen−oxygen and oxygen−hydrogen SDFs at several temperatures. They have verified the strong tendency for tetrahedral coordination of the nearest neighbors and compared their results with the approximate reconstruction of the pair distribution function from scattering experiments carried out by Soper.[19] Kusalik and co-workers[12,13] have also identified an interstitial feature responsible for the additional coordination in liquid water. Since this interstitial feature joins (bridges) the second and first coordination shells, it can be considered to be the consequence of the continually forming and collapsing local hydrogen bond network and therefore coupled to the mobility in the liquid.[12,13]

Figure 1 shows the oxygen−oxygen spatial distribution function of classical liquid water at 25 °C represented at the isosurface $g_{OO}(\mathbf{r}_{ij}) = 1.4$. The figure indicates the first and second neighbors features as well as the region associated with interstitial water. It is important to note that due to the existence of two symmetry planes (the molecular plane and a plane perpendicular to the molecule that contains the C_2 molecular axis) each feature is only labeled once in Figure 1. A central water molecule has been included to help in the visualization

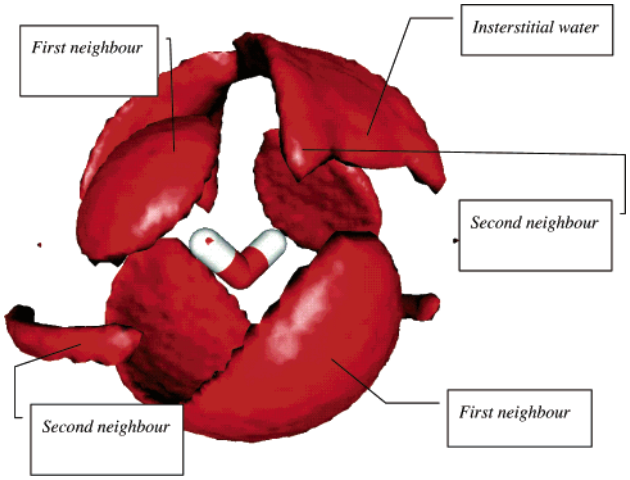

Figure 1. Oxygen−oxygen spatial distribution function of classical liquid water at 25 °C. The isosurfaces correspond to a threshold of 1.4, that is the enclosed regions have average oxygen densities at least 1.4 times that of the bulk. The central molecule defining the local frame has been included.

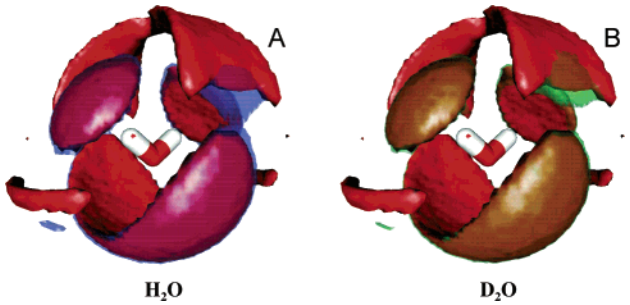

Figure 2. (A) Superposition of the oxygen−oxygen spatial distribution functions of classical water (red) and quantum liquid H_2O (semitransparent blue) at 25 °C. (B) Superposition of the oxygen−oxygen spatial distribution functions of classical water (red) and quantum liquid D_2O (semitransparent green) at 25 °C. All isosurfaces correspond to a threshold of 1.4, that is the enclosed regions have average oxygen densities at least 1.4 times that of the bulk. The central molecule defining the local frame has been included.

of the local frame. The relationship between the interstitial coordination and the dynamics in liquid water has been directly tested within the context of classical MD simulations.[13] By artificially restricting the movement from a hydrogen donor to an interstitial position the self-diffusion coefficient was reduced roughly by a factor of 2, providing further evidence of the important role of interstitial water in water dynamics.

In Figure 2A we compare local oxygen density maps of quantum and classical liquid H_2O obtained at 25 °C. We observe that the first "hydrogen (H) bonded" neighbors, apparent as two caps over the hydrogens and a single cupped feature below the oxygen of the central molecule, are shifted slightly to larger separations in the quantum system but otherwise appear relatively unaffected. More importantly, in the quantum H_2O result the nontetrahedral (interstitial) feature extends downward and essentially bridges to the H-bond coordination from below the central molecule. The existence of this specific region of higher oxygen density in the quantum system is a direct result of effective barrier lowering[11] due to the orientational uncertainty of the water molecule. This behavior can also be identified as "effective tunneling" and is responsible for the enhanced dynamics observed for quantum H_2O in comparison with the classical liquid.[10,11] Thus, although quantization appears to have less influence on the well-known tetrahedral coordination of liquid water, it does significantly lower the barrier between a

Figure 3. Superposition of the oxygen−oxygen spatial distribution functions of classical (red) and quantum (semitransparent blue) liquid H_2O at −20 °C with an isosurface threshold of 1.13. Only the slice perpendicular to the plane of the central molecule is shown.

H-bonded neighbor and the nontetrahedral coordination of a molecule. Consequently, water molecules in the quantum liquid exhibit a greater propensity to make and break hydrogen bonds. This result also underlines the importance of nontetrahedral coordination in the structure and dynamics of water.[12,13,15,20,21]

In Figure 2B the superposition of local oxygen density maps for quantum and classical liquid D_2O at 25 °C are shown. We note that the classical SDFs in Figure 2A,B are identical as expected. The penetration of the oxygen density into the low-probability classical region is less pronounced in quantum D_2O than in quantum H_2O (cf. Figure 2A). This result is naturally in agreement with the smaller quantum mechanical uncertainty of D_2O, in comparison with H_2O, as well as the smaller impact of quantization on the dynamical behavior of liquid D_2O.[10]

As mentioned above, it has already been shown that the impact of quantization in liquid water increases as the temperature is decreased, especially in the dynamical properties.[9,11] For example, the diffusion constant obtained for quantum H_2O at −20 °C is more than 300% larger than the value of the corresponding classical liquid.[11] (Clearly, this result draws into question the use of classical simulations to study at least some aspects of the dynamics in low-temperature water.[22−24]) It is therefore instructive to explore structural impacts. Focusing on liquid H_2O at −20 °C, Figure 3 compares a selected slice of the classical and quantum local oxygen density maps. We observe that the effects are analogous to those seen at higher temperatures with the nearest neighbor features in the quantum system displaced slightly toward larger separations. The effective tunneling in the quantum result is clearly captured in Figure 3 as a distinct bridging region in front of and behind the plane of the molecule.

It should be noted that whereas the "model" experiments carried out in this study, where quantum and classical systems characterized by the same interaction potential are compared, have no direct experimental analogue, they are nonetheless extremely useful comparisons since they directly probe the effect of interest, as illustrated in Figures 2 and 3.

B. The Quantum Mechanical Uncertainty. Let us now consider the question: "how does the quantum mechanical uncertainty in liquid water change with temperature?". A typical reference on the subject (e.g., ref 25) will state that the quantum mechanical uncertainty in a particle's coordinates is expected to grow as temperature decreases (although this conjecture is strictly valid only for free or otherwise weakly interacting particles). Furthermore, it is known that the effects of quantization on the properties of liquid water grow as temperature decreases.[11]

In liquid water it is the small inertia moments of the molecule that give rise to the quantum mechanical uncertainty associated with the orientation of the molecule.[3,5,16] The simulation

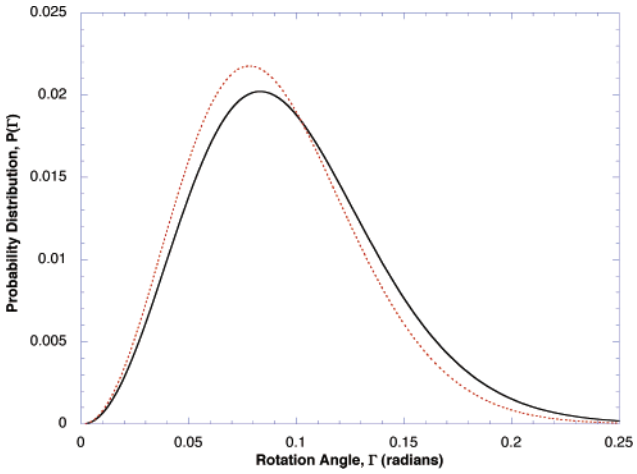

Figure 4. Quantum probability distribution functions for the molecular orientation of H_2O in ice Ih at −38 °C (dotted line) and liquid water at −35 °C (solid line). These normalized distributions are expressed in terms of the arc length (rotational angle about an arbitrary axis) Γ.

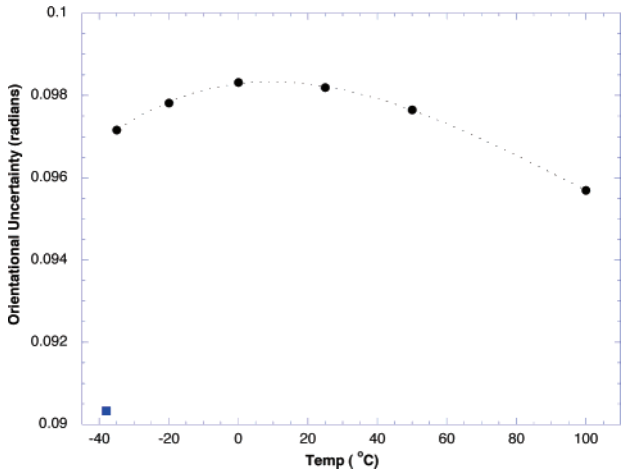

Figure 5. The average orientational uncertainty of the H_2O molecule in quantum liquid water as a function of temperature (dots). The values represent averages taken over the appropriate probability distribution function (as given in Figure 4). Included is a value obtained for ice Ih at −38 °C (square).

technique utilized in this study[10,16] effectively samples the orientational uncertainty for each molecule at each time step in the calculation. In such a simulation it is the orientational centroid (the orientation that corresponds to the average over the instantaneous quantum probability distribution of the molecular orientation) that is evolved in real time.[10,16] As a measure of the orientational uncertainty we have recorded the average quantum probability distribution function for molecular orientations about their centroids, which is given by

$$p(\Gamma) = \int dR \int d\Omega_c \rho_c(R,\Omega_c) \left\langle \delta\left(\Gamma - \frac{1}{P}\sum_{s=1}^{P}\Gamma(\Omega_s,\Omega_0)\right)\right\rangle_{\{\Omega_k\},\delta(\Omega_c-\Omega_0)} \quad (10)$$

except for an irrelevant constant factor. Figure 4 shows examples of two such functions (where, due to the homogeneity of the system, an average over all molecules has also been carried out). It should be noted that the expected Gaussian form of this quantum mechanical uncertainty is obtained[10,16] by taking into account the differential volume element of the rotation angle, $\sin^2(\Gamma/2)$.

According to eq 10, the two probability distributions given in Figure 4 represent the average quantum dispersion, or orientational blurring, for an H_2O molecule in ice Ih and liquid water. Clearly, the orientational uncertainty for an H_2O molecule is smaller in ice Ih than it is for liquid water at essentially the same temperature, suggesting a significant influence from the local environment on this molecular property. It should also be noted that (from integration of these quantum probability distribution functions) the orientational subspace necessary to account for 95% of the quantum probability is given by an arc length, Γ, approaching 12°. Alternatively, this value implies that any vector (such as the dipole or the OH bond) in the molecule is essentially distributed over a solid angle of about 0.13 rs (i.e. spans almost 10% of the surface of one octant of a sphere).

We have found that the shape of the quantum probability distribution functions for the molecular orientation in liquid H_2O systems is essentially unchanged over the temperature range −35 to 100 °C. It is convenient then to use simply the mean values of these distributions as a comparative measure of the orientational uncertainty,[10] i.e., $\langle\Gamma\rangle = \int \Gamma p(\Gamma) d\Gamma$. Figure 5 reports such average values for the H_2O molecule as a function of

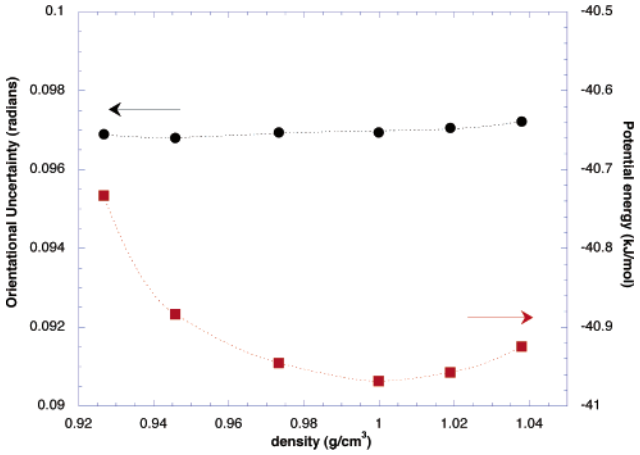

Figure 6. Dependence of the average orientational uncertainty (dots) and the average potential energy (squares) as a function of the density of liquid H_2O at −35 °C.

temperature. We observe the expected increase in the quantum mechanical uncertainty in going from 100 °C to about 0 °C. However, at this point the temperature dependence inverts and the uncertainty begins to decrease on further lowering of the temperature (i.e., in the range 0 to −35 °C). In view of our earlier discussion, this behavior is unexpected; furthermore, it may be described as a previously uncharacterized anomalous property of water. Since no attempt has been made in this study to reparametrize the TIP4P model for quantum simulations, it can be expected that the behavior recorded here will be shifted to somewhat lower temperatures relative to real water.

The behavior observed in Figure 5 appears to resemble the dependence of liquid water density with temperature. Since these data have been obtained from simulations[11] using experimental densities, one might suspect that the density is at least partially responsible for the observed curvature of the orientational uncertainty. However, Figure 6 demonstrates that the orientational uncertainty is not significantly affected by changes in density (at least over the range considered). The potential energy, on the other hand, does exhibit a shallow minimum at about 1.0 g/cm^3, consistent with previously observed behavior in classical simulations of liquid water.[18]

It might be suspected that water's unique structure plays at least some role in the unusual behavior observed in the

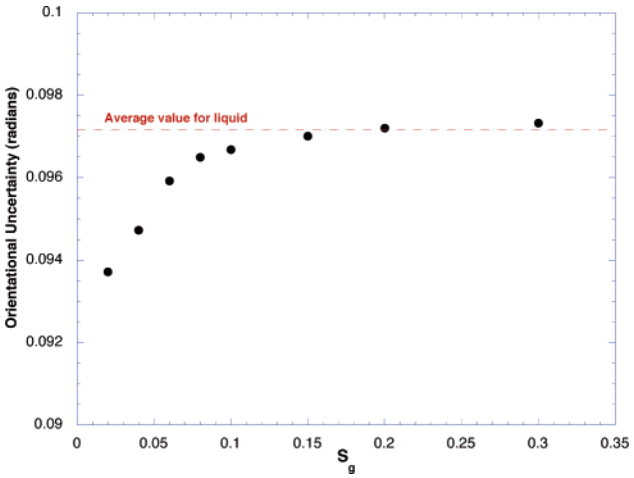

Figure 7. Dependence of the average orientational uncertainty in quantum liquid water as a function of the local structural parameter[26] S_g at −35 °C. The points represent averages taken over molecules with S_g values in the corresponding range. It should be noted that ice Ih has an average value for S_g of about 0.01. Similar behavior is observed at higher temperatures.

orientational uncertainty. The impact of the local molecular environment on the quantum mechanical uncertainty can be directly probed with a local tetrahedral order parameter. A convenient choice is the function[26] denoted S_g, where this order parameter, $0 \leq S_g \leq 1$, is small for molecules with tetrahedral (or icelike) arrangements of their four nearest neighbors. Utilizing this measure within a quantum simulation, the orientational uncertainty can be determined for molecules with the same (instantaneous) molecular environment according to

$$\langle \Gamma(\bar{S}_g) \rangle = \int \Gamma p(\Gamma, \bar{S}_g) d\Gamma \tag{11}$$

where for a system of N molecules

$$p(\Gamma, \bar{S}_g) = \int dR_1 \ldots \int dR_N \int d\Omega_{1,c} \ldots \int d\Omega_{N,c} \rho_c(R_1, \ldots, R_N, \Omega_{1,c}, \ldots, \Omega_{N,c}) \times \left\langle \sum_{i=1}^{N} \delta(\bar{S}_g - S_g(i)) \delta\left(\Gamma - \frac{1}{P}\sum_{s=1}^{P} \Gamma(\Omega_{i,s}, \Omega_{i,0})\right) \right\rangle_{\{\Omega_{i,k}\}, \delta(\Omega_{i,c} - \Omega_{i,0})} \tag{12}$$

with $S_g(i)$ being the S_g value for molecule i. We have evaluated this function for liquid water at several temperatures, and the results at −35 °C are shown in Figure 7. The histogram utilized for this figure is obtained for molecules with similar environments, i.e.

$$\langle \Gamma(S_g) \rangle = \frac{1}{\Delta S_g} \int_{S_g - \Delta S_g}^{S_g} \langle \Gamma(\bar{S}_g) \rangle d\bar{S}_g \tag{13}$$

From the results shown in Figure 7, it is clear that molecules in more icelike environments have a smaller orientational uncertainty than molecules in more disordered (or less tetrahedral) surroundings. This observation was also confirmed with the results of $\langle \Gamma(S_g) \rangle$ versus S_g obtained at higher temperatures that were very similar to the ones shown in Figure 7. Thus, the diminishing quantum mechanical uncertainty observed for liquid water with decreased temperatures (Figure 5) is due to the increasing influence of the molecular interaction potential that more than offsets the direct effect of lower temperature. In this case the local molecular structure in liquid water would play a key role in this behavior, as it does in other anomalous properties such as the density maximum exhibited by water.[12,27,28] Clearly, the results in Figure 7 also explain why the uncertainty of H_2O in ice Ih is smaller than in the liquid at the same temperature (see Figures 4 and 5).

IV. Conclusions

In this paper we probe the impact of quantization on the structure and dynamics of liquid water by comparing results of classical and quantum simulations of liquid water over a wide range of temperatures. An analysis based on the spatial distribution functions of classical and quantum liquid water has allowed us to describe explicitly the "effective tunneling" behavior in liquid H_2O and D_2O. We have shown that, when treated quantum mechanically, water molecules have an enhanced probability of accessing nontetrahedral coordination in the local three-dimensional structure. The relationship between "effective tunneling", hydrogen-bond breaking, and molecular diffusion has also been clarified.

Since quantum mechanics dictates that there is an uncertainty associated with determining the orientation of any water molecule, we have explored the behavior of this orientational "blurring" with temperature. We have shown that the local molecular environment affects the quantum mechanical uncertainty of the water molecules and leads to a nonmonotonic behavior. The results presented here are further evidence of the notable strength of the water−water interaction in condensed phase and the importance of water structure.

We have provided a clear demonstration of the significant role quantization of molecular motion can play in the physical properties of liquid water. Indeed, very recent observations[29] of extremely fast loss in the frequency correlation or memory of structural variations in the hydrogen bond network of pure H_2O, as opposed to much longer correlations in D_2O, supports our prediction of quantum effects enhancing the rotational motion of H_2O molecules. Work is now under way[30] to see if the temperature dependence reported here can be detected in these experiments.

Finally, we note that results from quantum simulations of liquid water and ice comparing several water models will appear elsewhere;[31] it is important to point out that the observations made there confirm the conclusions in this work. Moreover, a more extensive study of quantum effects on TIP4P ice will also be described elsewhere.[32]

Acknowledgment. We are grateful for the financial support of the Natural Sciences and Engineering Research Council of Canada.

References and Notes

(1) Eisenberg, D.; Kauzmann, W. *The Structure and Properties of Water;* Oxford University Press: Oxford, 1969.
(2) Svishchev, I. M.; Kusalik, P. G. *J. Phys. Chem.* **1994**, *98*, 728.
(3) Kuharski, R. A.; Rossky, P. J. *J. Chem. Phys.* **1985**, *82*, 5164.
(4) Wallqvist, A.; Berne, B. J. *Chem. Phys. Lett.* **1985**, *117*, 214.
(5) del Buono, G. D.; Rossky, P. J.; Schnitker, J. *J. Chem. Phys.* **1991**, *95*, 3728.
(6) Stern, H. A.; Berne, B. J. *J. Chem. Phys.* **2001**, *115*, 7622.
(7) Lobaugh, J.; Voth, G. A. *J. Chem. Phys.* **1997**, *106*, 2400.
(8) Schwegler, E.; Grossman, J. C.; Gygi, F.; Galli, G. *J. Chem. Phys.* **2004**, *121*, 5400.
(9) Guillot, B.; Guissani, Y. *J. Chem. Phys.* **1998**, *108*, 10162.
(10) Hernández de la Peña, L.; Kusalik, P. G. *J. Chem. Phys.* **2004**, *121*, 5992.
(11) Hernández de la Peña, L.; Kusalik, P. G. *J. Am. Chem. Soc.* **2005**, *127*, 5246.
(12) Kusalik, P. G.; Svishchev, I. M. *Science* **1994**, *265*, 1219.

(13) Kusalik, P. G.; Laaksonen, A.; Svishchev, I. M. In *Molecular Dynamics. From Classical to Quantum methods;* Balbuena, P. B., Seminario, J. M., Eds.; Elsevier: Amsterdam, 1999; pp 61−97.

(14) Cao, J.; Voth, G. A. *J. Chem. Phys.* **1993**, *99*, 10070. Cao, J.; Voth, G. A. *J. Chem. Phys.* **1994**, *100*, 5093. Cao, J.; Voth, G. A. *J. Chem. Phys.* **1994**, *100*, 5106. Cao, J.; Voth, G. A. *J. Chem. Phys.* **1994**, *100*, 6157. Cao, J.; Voth, G. A. *J. Chem. Phys.* **1994**, *100*, 6168. Jang; S.; Voth, G. A. *J. Chem. Phys*. **1999**, *111*, 2357. Jang; S.; Voth, G. A. *J. Chem. Phys*. **1999**, *111*, 2371.

(15) Svishchev, I. M.; Kusalik, P. G. *Chem. Phys. Lett.* **1994**, *215*, 596.

(16) Hernández de la Peña, L.; Kusalik, P. G. *Mol. Phys.* **2004**, *102*, 927.

(17) Jorgensen, W. L.; Chandrasekhar, J.; Madura, J. D.; Impey, R. W.; Klein, M. L. *J. Chem. Phys.* **1983**, *79*, 926.

(18) Poole, P. H.; Sciortinio, F.; Essmann, U.; Stanley, H. E. *Phys. Rev. E* **1993**, *48*, 3799.

(19) Soper, A. K. *J. Chem. Phys.* **1994**, *101*, 6888. Soper, A. K. *Physica B (Amsterdam)* **1995**, *214*, 448.

(20) Sciortino, F.; Geiger, A.; Stanley, H. E. *Nature* **1991**, *354*, 218.

(21) Geiger, A.; Kleene, M.; Paschek, D.; Rehtanz, A. *J. Mol. Liq*. **2003**, *106*, 131.

(22) Scala, A.; Starr, F. W.; La Nave, E.; Sciortino, F.; Stanley, H. E. *Nature* **2000**, *406*, 166.

(23) Debenedetti, P. G.; Stanley, H. E. *Phys. Today* **2003**, *56*, 40.

(24) Starr, F. W.; Angell, C. A.; La Nove, E.; Sastry, S.; Scala, A.; Sciortino, F.; Stanley, H. E. *Biophys. Chem.* **2003**, *105*, 573.

(25) Chandler, D. *Introduction to modern Statistical Mechanics*; Oxford University Press: New York, 1986.

(26) Chau, P. L.; Hardwick, A. J. *Mol. Phys.* **1998**, *93*, 511.

(27) Errington, J. R.; Debenedetti, P. G. *Nature* **2001**, *409*, 318.

(28) Billeter, S. R.; King, P. M.; van Gunsteren, W. F. *J. Chem. Phys.* **1994**, *100*, 6692.

(29) Cowan, M. L.; Bruner, B. D.; Huse, N.; Dwyer, J. R.; Chugh, B.; Nibbering, E. T. L.; Elsaesser, T.; Miller, R. J. D. *Nature* **2005**, *434*, 199.

(30) Miller, R. J. D., private communication.

(31) Hernández de la Peña, L.; Gulam Razul, M. S.; Kusalik, P. G., to be submitted.

(32) Hernández de la Peña, L.; Gulam Razul, M. S.; Kusalik, P. G. *J. Chem. Phys*., submitted for publication, June, 2005.